Proceedings of the 21st ICSMGE, Vienna, Austria, 14 – 19 June 2026. Pistrol, Adam & Schweiger (eds.)
Published by: ÖGG, Austrian Society for Geomechanics, Salzburg, Austria, ISBN 978-3-9503898-4-5
https://doi.org/10.53243/ICSMGE2026-964

Application of the Convected Particle Domain Interpolation method in modelling offshore vibratory monopile installation

Shreyas Giridharan
Institute of Geotechnical Engineering, University of Stuttgart, Germany, shreyas.giridharan@igs.uni-stuttgart.de

Dieter Stolle
Faculty of Civil Engineering, McMaster University, Hamilton, Ontario, Canada

Christian Moormann
Institute of Geotechnical Engineering, University of Stuttgart, Germany

ABSTRACT: The global push toward clean energy has been strongly supported by the increasing deployment of offshore wind farms. In these systems, monopiles are commonly used as foundation elements. While impact-driven installation remains standard practice, vibratory driving is gaining interest due to its shorter installation time, lower underwater noise levels, and reduced fatigue loading on the monopile. However, a detailed understanding of the soil-structure interaction during vibratory installation is still limited. Numerical simulation offers an effective way to investigate these processes. In this work, the Convected Particle Domain Interpolation (CPDI) method, an enhanced version of the Material Point Method, is used to perform dynamic simulations of monopile installation. The model includes a two-phase formulation to represent saturated soil behaviour, along with a multi-layer soil profile calibrated using site-specific data. The simulation tool has been validated against field data from full-scale installations. Results from vibratory and impact-driven monopile installations at the KASKASI-II offshore wind farm in the North Sea are presented. The study analyses the influence of installation frequency and applied hook load on the driving process. In addition, wave propagation through the seawater column, generated by the pile and soil movement, is modelled and compared to field measurements. For this purpose, the simulation was extended to include a water domain interacting with both the monopile and the saturated seabed. The findings contribute to a better understanding of installation dynamics and hydrodynamic effects relevant to offshore wind foundation design and planning.

KEYWORDS: offshore geotechnics, monopile installation, convected particle domain interpolation method, material point method.

1 INTRODUCTION

As the global energy sector moves toward more sustainable alternatives to combat climate change, wind energy has emerged as a key solution, offering both long operational lifespans and low maintenance demands. Within offshore wind infrastructure, monopile foundations dominate the industry, comprising nearly 80 % of existing installations (Gupta & Basu, 2020). Their widespread use is largely attributed to the straightforward nature of their design, fabrication, and deployment processes (Ho et al., 2016). With respect to installation techniques, two primary methods are in use: impact driving and vibratory driving. While the mechanics and post-installation strength of impact-driven installation are well documented, vibratory driving remains less understood, leading to hesitancy in its broader adoption despite its potential for reducing installation time and costs.

This study focuses on improving the understanding of vibratory monopile installation using a numerical approach based on the two-phase Convected Particle Domain Interpolation (CPDI) method, an advancement over the classical Material Point Method (MPM). To accurately simulate the behaviour of sandy seabed soils, the model uses the UBCSAND constitutive model. Site-specific cone penetration test (CPT) data is used to generate a layered soil continuum, allowing the simulation to reflect variations in relative density with depth. The paper also explores how different driving parameters affect both the final embedded depth and the installation rate of the monopile.

Beyond soil-structure interaction, the study also considers fluid-structure effects by incorporating a free-water model into the simulation. This model captures the generation and propagation of pressure waves in the water column during installation, accounting for interactions between the monopile, the surrounding soil, and the seawater. The resulting simulation framework offers a practical tool for offshore wind developers to predict installation behaviour and optimize project planning for future monopile-based foundation systems.

2 THE CONVECTED PARTICLE DOMAIN INTERPOLATION (CPDI) METHOD

2.1 *Numerical formulation of the CPDI method*

The numerical approach employed in this study is the Material Point Method (MPM), a particle-based computational framework originally proposed by Sulsky & Schreyer (1996). MPM is particularly well suited for large deformation problems, as it combines the strengths of both Lagrangian and Eulerian methods. In this approach, the physical domain is represented by Lagrangian points, also referred to as material points or particles, which move through a fixed Eulerian mesh known as the background grid. Each particle stores essential physical quantities such as mass, momentum, stress, strain, and other internal state variables.

The incremental solution is carried out on the background grid following a Lagrangian approach. Once the calculation on the grid is completed, the updated values are transferred back to the particles to update their values and their state. The background grid is then cleared, ready for the next time step. This framework enables MPM to leverage the advantages of both Lagrangian and Eulerian formulations, while minimizing their individual drawbacks.

Despite its advantages, the classical MPM suffers from numerical instabilities, particularly when particles cross from one grid cell to another. This issue is more pronounced when linear shape functions are used, as they produce discontinuous gradients at cell boundaries. While the use of higher-order shape functions can reduce this error, it comes at the cost of increased computational complexity. To address these limitations, several improved formulations have been developed over time. One such improvement is the Convected Particle Domain Interpolation (CPDI) method, adopted in this

work, which mitigates grid-crossing errors by distributing the particle mass over a finite subdomain rather than concentrating it at a single point, as schematically illustrated in Figure 1, where the different material point domain representations in the MPM variants considered here are compared. By representing each material point with a finite domain, CPDI provides a smoother transfer of kinematic quantities between particles and grid and offers a more stable and robust basis for the large-deformation monopile installation analyses carried out in this study.

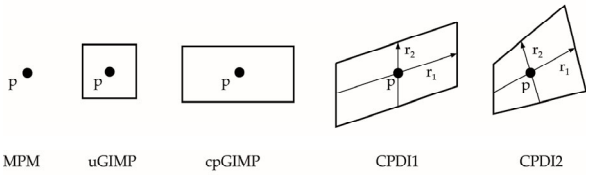

Figure 1. Representation of the different MPM version domains.

For a detailed explanation of the MPM framework, readers may refer to Giridharan (2022), and for an in-depth treatment of the CPDI method, see (Sadeghirad et al., 2011).

2.2 *Two-phase formulation of CPDI method*

In order to accurately simulate saturated soils, it is necessary to account for hydro-mechanical interactions between the pore water (liquid phase) and the solid skeleton (solid phase). The two-phase formulation implemented in this study is based on the work described in Kafaji (2013), which provides a detailed theoretical foundation for modelling such interactions. Readers seeking a comprehensive numerical treatment of the two-phase approach implemented within the MPM framework are encouraged to consult that reference. Readers are referred to Chan et al. (2022) for a more general numerical treatment of porous media within the context of soil mechanics. For completeness, this work includes only the key equations necessary to describe the behaviour of two-phase media relevant to the present study.

Solid phase mass conservation is described by the equation:

$$\frac{d}{dt}\left[(1-n)\ \rho_s\right] + \frac{\partial}{\partial x_j}\left[(1-n)\,\rho_s\,\widehat{v_j}\right] = 0, \tag{1}$$

where, $\widehat{v_j}$ is the velocity vector of the solid phase. The mass conservation relationship for the water phase is as follows:

$$\frac{d}{dt}\left[(n\ \ \rho_w)\right] + \frac{\partial}{\partial x_j}\left[n\,\rho_w\,\widehat{w_j}\right] = 0, \tag{2}$$

where, $\widehat{w_j}$ is the vector of true velocity of the water phase. The variables n, ρ_w and ρ_s are the porosity, density of water and solid grains, respectively. The following two assumptions are adopted in the subsequent formulation:

1. soil grains are treated as incompressible, and
2. spatial variations in porosity and density within the control mass are neglected.

Assuming water is linearly compressible and rearranging the governing equations leads to the storage equation, which serves as the constitutive relation for the pore fluid:

$$\frac{d\,p}{d\,t} = \frac{K_w}{n}\left[(1-n)\ \frac{\partial\,\widehat{v_j}}{\partial\,x_j} + n\ \frac{\partial\,\widehat{w_j}}{\partial\,x_j}\right], \tag{3}$$

where, p is the pore pressure and K_w is the bulk modulus of water. Treatment of soil-structure interaction

2.3 *Treatment of soil-structure interaction*

Previous studies, such as (Bardenhagen et al., 2001), focused on relaxing the no-slip and no-separation contact conditions. To improve the contact algorithm, Hamad et al. (2017) introduces the penalty function method for computing contact forces between interacting bodies. In this method, the surface of the continuum is discretized independently from the volume, as opposed to contact treatment happening directly between the particles. This allows better representation of boundary interactions. By assigning a small mass to the one-dimensional, two-noded linear contact interface segments, they are able to follow the deformation of the material that they are attached to. Based on the equations of motion, surface nodes from different bodies can interact through the penalty function. Frictional effects are then incorporated as external contact forces applied along the boundary.

In this method, the penalty-based penalization for contact is used. In the penalty function method, if a region Γ_c where contact violation exists, the potential energy is penalised proportional to the amount of constraint violation by using a penalty function P, expressed as:

$$P = \frac{1}{2}\,\omega_n \int_{\Gamma_c} g^2{}_n\, d\Gamma_c + \frac{1}{2}\,\omega_t \int_{\Gamma_c} g^2{}_t\, d\Gamma_c, \tag{4}$$

where, ω is the penalty parameter, g is the gap function, and the subscripts n and t are the normal and tangential directions, respectively.

These elements are also assigned a normal and tangential stiffness values, which serve as penalty parameters within the formulation. Building on this method, further developments have incorporated penalty-based friction models and successfully applied them to geotechnical problems such as pile installation, as demonstrated in the studies by Giridharan et al. (2020) and Giridharan (2022).

3 NUMERICAL TREATMENT OF OFFSHORE MONOPILE INSTALLATION

The Convected Particle Domain Interpolation code has been previously used to simulate both solid piles (Hamad, 2016) and open-ended steel pipe pile installation processes (Giridharan, 2022). Moormann et al. (2018) and Moormann et al. (2019) extended the CPDI framework to model the pile installation in a fully-couple saturated sand framework, using the hypoplastic soil model (Niemunis & Herle, 1997). Later, Giridharan et al. (2019) incorporated the UBCSAND constitutive model (Naesgaard, 2011) into the CPDI code to capture the effects of liquefaction during dynamic installation and applied this enhanced model to simulate pile driving scenarios.

This study presents the results of a Class-A (pre-event) prediction of monopile installation depth. The objective was to evaluate the installation behaviour of monopiles driven by vibratory methods before actual offshore deployment, with the aim of estimating the time required for installation. The predicted results are later compared with field measurements to assess the accuracy and reliability of the simulation tool for offshore applications.

In addition, the study investigates the influence of key parameters on the installation rate, focusing on the driving frequency and stratified soil layers with different relative densities. An initial attempt is also made to model the interaction between seawater (represented as free water) and the saturated soil, allowing simulation of pressure wave propagation through the water column during the vibratory installation process.

4 MONOPILE VIBRATION SIMULATION

The numerical model is based on an axially symmetric formulation and incorporates the penalty contact algorithm, the two-phase CPDI framework, and the UBCSAND constitutive model. The UBCSAND model, which has previously been applied to both model-scale and full-scale pile installation tests, demonstrated good agreement in Class-C (back-analysis) simulations. In this study, the model is used for Class-A (pre-event) predictions, which are inherently more demanding. Unlike back-calculations, Class-A simulations require estimation of soil parameters directly from cone penetration test (CPT) data, without the benefit of calibration against known outcomes.

4.1 *Dimensions of the model and discretization*

To construct a model capable of simulating the dynamic pile installation process within a reasonable computational timeframe, a number of assumptions are necessary. Specifically:

1. the soil is assumed to be fully saturated,
2. the pile is considered to have a constant cross-section, and
3. the soil is treated as homogeneous and isotropic.

The soil behaviour is represented using a single, averaged parameter set distributed uniformly across the domain. This simplification is primarily due to the limited availability of high-quality soil test data. Since detailed laboratory testing was not available for the site, further refinement of model parameters could not be justified. These assumptions provide a practical basis for conducting forward predictions using available CPT data.

The axisymmetric domain shown in Figure 2, which includes both the soil and pile continua, was discretized using approximately 27,000 material points and 13,000 interface elements to model the pile-soil interaction. The computational background grid employed a tartan mesh configuration, with the smallest grid cells measuring 0.1 m by 0.01 m. Prior to the start of the simulation, the pile was pre-embedded to a depth of five meters. This initial embedment was selected partly to enhance numerical stability, as the depth of penetration due to self-weight could not be reliably predicted in advance.

4.2 *Initial Conditions*

The vibration process in the field began at a pile height of 34.8 metres, which translates to a self-weight penetration of 2.2 metres. The numerical simulation, however, assumed a self-penetrating depth of 5 metres. This assumption was made in part to improve the numerical robustness of the CPDI code, as instability in the calculation process has been observed when applying dynamic load at lower effective stress regimes. However, this decision was deliberate and not the result of calculations. The effective stresses were assigned to the particles using the K_0 procedure, and a 5-second quasi-static step, in which no dynamic load was applied to achieve a steady-state condition, was performed on the model.

Given the similarity in soil characteristics and geological history between the Cuxhaven region and the intended offshore wind farm location, the UBCSAND parameters calibrated for Cuxhaven sand, as listed in Table 1, were adopted for modelling the soil continuum. The availability of high-quality laboratory data for this site allowed for accurate parameter calibration, and the parameters were calibrated to a relative density of 100%, based on the evaluation of the CPT data. For modelling the fluid in the fluid-saturated sand, a full bulk modulus value of 2 GPa and a permeability value, k of 1×10^{-4} m/s was assumed.

Table 1. UBCSAND model parameters for Cuxhaven Sand.

$N1_{60}$[-]	m_e[-]	n_e[-]	n_p[-]	K_G^E[-]	K_B^E[-]
10.7	0.7	0.7	0.4	100	125
K_G^P[-]	ϕ_{pt}[°]	ϕ_f[°]	c[kPa]	Pa[kPa]	σ_t[kPa]
5	31	31.1	0	100	0
$hfac_1$[-]	$hfac_2$[-]	$hfac_3$[-]	$hfac_4$[-]	$hfac_5$[-]	$hfac_6$[-]
0.65	0.85	1.0	0.6	1.0	0.95

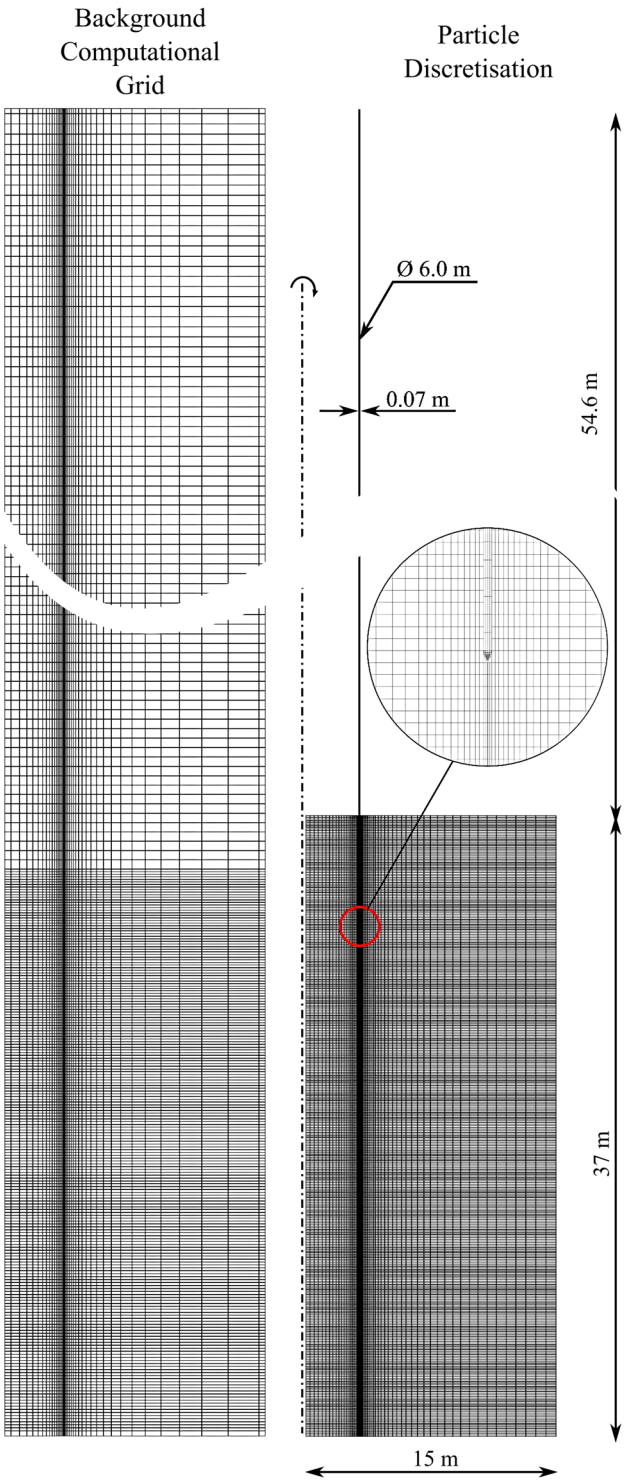

Figure 2. Background computational grid discretisation (left), and Particle discretisation of pile and soil (right).

The modelled pile has an outer diameter of 6.0 m, an average wall thickness of 70 mm, a total length of 59.62 m, and a mass of 646.6 tons. The vibrator parameters used in the installation simulation are provided in Table 2. The dynamic loading was applied at the pile head. During the simulation, the static component of the load remained constant, while the dynamic component followed a sinusoidal variation at the frequency specified in the table. The pile was modelled using the mechanical properties of steel, with a Young's modulus of 200 GPa and a Poisson's ratio of 0.3. Contact elements along the pile-soil interface were assigned a friction coefficient of 0.4. This value was selected to represent the expected pile-soil interface resistance for the very dense sand at the project site and lies within the typical range reported for dense to very dense sand with a relatively smooth steel pile.

Table 2. Vibrator parameters.

Parameter	Value
Frequency of Vibrator	20 Hz
Total mass, with mounting elements	435 tons
Static load	4,266 kN
Dynamic load	30,319 kN

4.3 *Initial installation results*

Figure 3 compares the numerically predicted and measured penetration curves for the monopile installation. The results indicate that the simulation using the UBCSAND model effectively captures both the qualitative behaviour of the installation process and the final embedment depth observed in the field. While the early stages of the simulation show strong agreement with the measured installation rate, a slight deviation emerges as the penetration progresses.

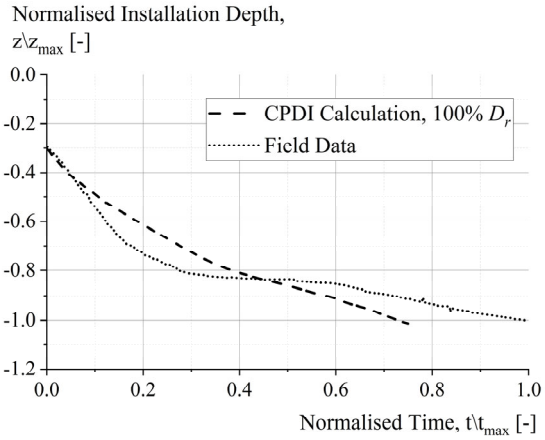

Figure 3. Class-A prediction results of monopile installation.

Two key outcomes underscore the performance of the numerical model:

1. the simulation successfully reproduces the final penetration depth achieved during offshore vibratory installation, and
2. the model maintains numerical stability throughout the dynamic simulation.

Furthermore, the gradual reduction in installation rate, attributed to increasing shaft friction and soil resistance, suggests that the model realistically accounts for the evolving interaction between the pile and surrounding soil during the driving process.

4.4 *Layered subsoil simulation*

To represent the variation in soil properties with depth, a two-layer soil model was implemented into the CPDI code as an initial step. Although both layers were governed by the same constitutive model, namely UBCSAND, distinct sets of parameters were assigned to each layer to more accurately compute the effective stress responses. In principle, this framework can be extended to include multiple layers; however, the effort required for parameter calibration increases proportionally with the number of layers introduced. The two-layer configuration presents a practical starting point for this study, as only two relative density values were clearly distinguishable across the depth range of interest based on available site data.

Within this framework, two key goals were established for the CPDI-based simulations:

1. to replicate the pile penetration behaviour observed in the field as closely as possible, and
2. to simulate the maximum embedment depth reached during actual offshore installation.

Figure 4 shows the simulation results obtained using the UBCSAND model for the layered soil profile. Compared to a uniform soil model assuming 100% relative density, the two-layer model demonstrates a noticeably faster installation rate up to a normalized depth of $z/z_{max} = 0.8$. In this upper region, the soil was defined with a relative density of 75%. Below this depth, the penetration rate decreases significantly. In the layered simulations, the UBCSAND parameters listed in Table 1 were adapted between the upper and lower layers by assigning a set of different values of the state and stiffness parameters. For the 75% D_r layer, $N1_{60}$ was reduced to 8.5, K_G^E and K_B^E were reduced to 90 and 110, respectively. The remaining material constants were kept identical for both layers.

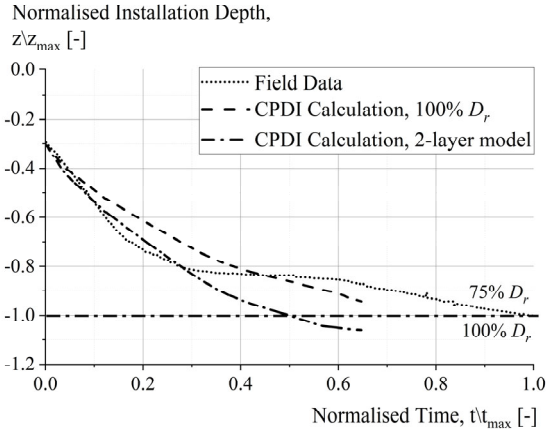

Figure 4. Installation process with two subsoil layers.

This reduction in installation speed is primarily attributed to two factors:

1. the increase in shaft friction as the pile advances deeper into the denser soil layer, and
2. the rise in oedometer stiffness associated with the lower layer.

The elevated stiffness is not only a result of the higher relative density but also reflects the nonlinear increase in stiffness relative to the evolving stress state, which is explicitly accounted for within the UBCSAND formulation.

4.5 *Effect of vibrator frequency on the installation rate*

In the context of offshore monopile installation, the term "driving frequency" refers to the rate at which vibratory loads are applied to the pile during its penetration into the seabed. This parameter plays a critical role in determining the effectiveness and efficiency of the installation process.

Generally, an increase in driving frequency leads to enhanced energy transfer to the pile-soil system, which often results in improved soil displacement and deeper penetration within a given timeframe. As such, careful selection of the driving frequency is essential to optimize installation performance. The optimal frequency must account for several influencing factors, including soil stratigraphy and stiffness, pile geometry, and the technical limitations of the installation equipment.

Figure 5 illustrates the impact of driving frequency on installation behaviour, based on simulations performed using the UBCSAND constitutive model. The simulation results show a clear trend: higher frequencies are associated with faster installation rates. This trend aligns with theoretical expectations, as greater vibratory energy is imparted to the system when the frequency increases, thereby facilitating pile advancement.

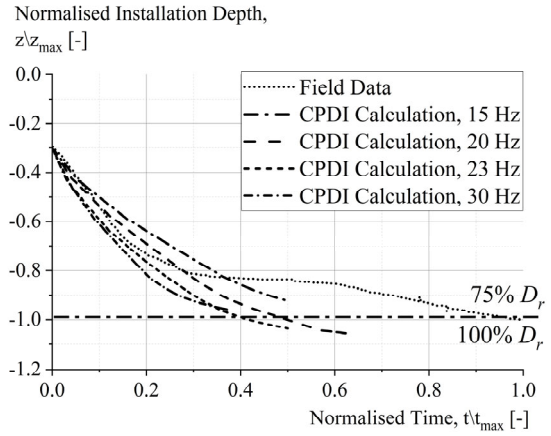

Figure 5. Effect of vibrator frequency on installation rate.

However, the results also reveal a more complex behaviour at deeper penetration levels. At a frequency of 30 Hz, the installation rate begins to decline at greater depths compared to the response observed at 23 Hz. This observation suggests that while higher frequencies may enhance performance in the upper layers, they may also contribute to increased soil resistance at deeper levels. One plausible explanation, as suggested in previous work by Bakroon (2020), is that the effective stress in the soil surrounding the pile becomes more pronounced under higher-frequency loading. This increase in effective stress leads to stiffer soil response and, consequently, greater resistance to further penetration. These findings highlight the need for a balanced selection of driving frequency, tailored to both the soil profile and the installation depth, to ensure efficient and controlled pile driving.

4.6 *Comparison of numerical simulation with hydroacoustical field data*

The comparison between field-recorded sound pressure level (SPL) measurements and simulation results involves a technical adjustment due to practical modelling constraints. In the field, SPL measurements were taken at a horizontal distance of 90 meters from the pile installation site. Simulating a full-scale domain of that width, including both saturated soil and seawater, would have significantly increased computational costs and exceeded the available project timeline. To address this limitation, a reduced domain width of 15 meters was implemented in the numerical model, with absorbing boundary conditions applied at the lateral edges to minimize artificial wave reflections.

Because of the discrepancy in measurement and simulation distances, a correction was applied to align the field data with the simulation setup. Specifically, an empirical correction factor of 7.5 dB was added to the measured SPL values to approximate the sound pressure at a distance of 7.5 meters, the location in the model where SPL was evaluated. This correction factor is based on previously published field measurements and provides a reasonable basis for adjusting the field data for comparison.

Following this adjustment, the SPL values were converted from decibels [dB] to pressure units [kPa] to allow for a direct comparison with the simulation output. The following standard formula was used for the conversion between [dB] and [kPa]:

$$1\ kPa = 10^{\left(\frac{Lp|dB|}{20}\right)} \cdot 10^{-9}, \tag{5}$$

Given the uncertainties inherent in field measurements, such as the exact placement of the hydrophone, background environmental noise, vessel orientation, and other external factors, it is more appropriate to compare simulation results against an averaged SPL value rather than isolated peaks. The simulation outputs were therefore evaluated relative to this averaged measurement, as presented in Figure 6.

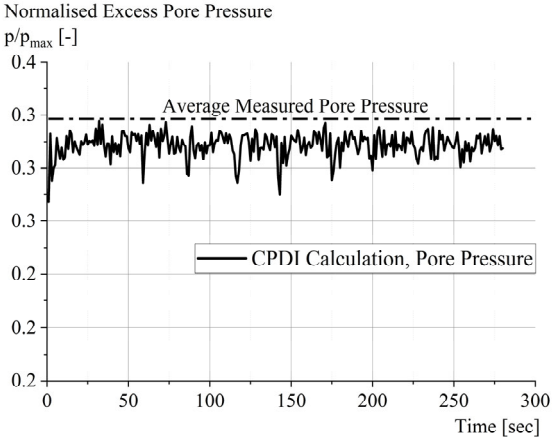

Figure 6. Numerically calculated normalized hydroacoustic pressure compared against averaged measured pressure in seawater.

Even with the inclusion of necessary modelling assumptions, the CPDI-based simulation is able to reproduce the observed pressure range associated with the installation process with reasonable accuracy. This demonstrates the capability of the model to capture key hydrodynamic features of the offshore monopile installation.

It should be noted, however, that while the implementation of absorbing boundaries significantly reduces artificial wave reflections at the edges of the domain, it does not eliminate them entirely. Some residual reflections may still occur and propagate back into the soil-water continuum. It is assumed that the interaction between these reflected waves and the primary waves generated by the monopile contributes to the minor pressure fluctuations observed in the simulation results. These effects are inherent to the modelling strategy and should be considered when interpreting the pressure data.

5 CONCLUSIONS

This study demonstrates the application of the Convected Particle Domain Interpolation (CPDI) method for simulating the vibratory installation of offshore monopiles, using a two-phase formulation to model saturated soil behaviour. The integration of the UBCSAND constitutive model enabled the representation of realistic sand response, including the effects of relative density variation, pore pressure development, and stiffness evolution under cyclic loading. The framework also included fluid-soil interaction by coupling free water with the

saturated soil domain, allowing for the simulation of pressure wave propagation during installation.

A Class-A prediction was performed to assess the ability of the model to forecast installation behaviour without prior calibration to field results. Despite the simplified soil layering and limited calibration data, the simulation reproduced the measured penetration depth with reasonable accuracy and maintained numerical stability throughout the dynamic loading process. The model effectively captured key phenomena such as reduced installation rates with increasing depth, which were attributed to higher shaft resistance and increased stiffness in deeper, denser soil layers.

Parametric studies confirmed the sensitivity of installation rate to vibratory frequency, showing that higher frequencies enhance penetration efficiency in upper soil layers but may induce increased resistance at depth due to elevated effective stresses. The inclusion of absorbing boundaries and a domain correction strategy enabled a meaningful comparison of hydroacoustic pressure levels between simulation and field measurements. Although some fluctuations were observed due to wave reflection interactions, the model successfully reproduced the overall pressure range measured in the field.

The CPDI-based framework presented here provides a robust and flexible tool for predicting monopile installation behaviour under vibratory loading. It enables offshore engineers to evaluate installation performance and hydroacoustic impacts prior to field deployment. The ability to conduct Class-A predictions using limited input data demonstrates the potential of this method for planning and optimizing foundation installation in offshore wind energy projects.

Future work may focus on improving the calibration of soil parameters from in-situ and laboratory data, extending the model to fully three-dimensional configurations, and incorporating more refined descriptions of equipment-soil interaction, particularly under variable loading conditions and heterogeneous soil profiles.

6 ACKNOWLEDGEMENTS

A portion of the results presented in this work was supported by the project ‘VISSKA- Measurement, modelling and assessment of vibratory pile driving in relation to installation, noise emissions and effects on harbour porpoises at the KASKASI II offshore wind farm’ under grant number 03EE3034D. The authors would like to acknowledge the funding from the German Federal Ministry for Economic Affairs and Climate Action (BMWK), and Projektträger Jülich (PtJ) for the project management support.

7 REFERENCES

Bakroon, M., 2020. Employment of a Multi-Material ALE approach using nonlinear soil models to simulate large deformation geotechnical problems. Doctoral dissertation. Berlin: Technische Universität Berlin.

Bardenhagen, S. G., Guilkey, J. E., Roessig, K. M., Brackbill, J. U., Witzel, W. M., & Foster, J. C. , 2001. An improved contact algorithm for the material point method and application to stress propagation in granular material. Computer Modelling in Engineering and Sciences, 2(4), pp.509–522.

Chan, A.H., Pastor, M., Schrefler, B.A., Shiomi, T. & Zienkiewicz, O.C., 2022. Computational geomechanics: theory and applications. Hoboken, NJ: John Wiley & Sons.

Giridharan, S., 2022. Convected Particle Domain Interpolation Method for Large Deformation Geotechnical Problems. Doctoral dissertation. Stuttgart: Institut für Geotechnik, Universität Stuttgart.

Giridharan, S., Gowda, S., Stolle, D. F. E. & Moormann, C., 2020. Comparison of UBCSAND and Hypoplastic soil model predictions using the Material Point Method. Soils and Foundations, 60(4), pp.989–1000.

Giridharan, S., Stolle, D. & Moormann, C., 2019. Modelling liquefaction using the material point method–an evaluation using two constitutive models. Proceedings of the 2nd International Conference on the Material Point Method for Modelling Soil-Water-Structure Interaction, 8–10 January 2019, Churchill College, Cambridge, United Kingdom.

Gupta, B. K. & Basu, D., 2020. Offshore wind turbine monopile foundations: Design perspectives. Ocean Engineering, Volume 213, pp.107514.

Hamad, F., 2016. Formulation of the axisymmetric CPDI with application to pile driving in sand. Computers and Geotechnics, 74, pp.141–150.

Hamad, F., Giridharan, S. & Moormann, C., 2017. A penalty function method for modelling frictional contact in MPM. Procedia Engineering, 175, pp.116–123.

Ho, A., Mbistrova, A. & Corbetta, G., 2016. The European offshore wind industry-key trends and statistics 2015. Brussels: European Wind Energy Association.

Kafaji, I. K., 2013. Formulation of a dynamic material point method (MPM) for geomechanical problems. Doctoral dissertation. Stuttgart: Universität Stuttgart.

Moormann, C., Gowda, S. & Giridharan, S., 2018. Numerical simulation of pile installation in saturated soil using CPDI. Proceedings of the 9th European Conference on Numerical Methods in Geotechnical Engineering (NUMGE 2018), 25–27 June 2018, Porto, Portugal. Leiden: CRC Press,1, pp.665–672.

Moormann, C., Gowda, S. & Giridharan, S., 2019. Numerical simulation of open-ended pile installation in saturated sand. Proceedings of the 17th European Conference on Soil Mechanics and Geotechnical Engineering (ECSMGE 2019), 1–6 September 2019, Reykjavik, Iceland. Leiden: CRC Press, pp.459–466.

Naesgaard, E., 2011. A hybrid effective stress–total stress procedure for analyzing soil embankments subjected to potential liquefaction and flow. Doctoral Dissertation. Vancouver: The University of British Columbia (Canada).

Niemunis, A. & Herle, I., 1997. Hypoplastic model for cohesionless soils with elastic strain range. Mechanics of Cohesive-frictional Materials: An International Journal on Experiments, Modelling and Computation of Materials and Structures, 2(4), pp.279–299.

Sadeghirad, A., Brannon, R. M. & Burghardt, J., 2011. A convected particle domain interpolation technique to extend applicability of the material point method for problems involving massive deformations. International Journal for numerical methods in Engineering, 86(12), pp.1435–1456.

Sulsky, D. & Schreyer, H. L., 1996. Axisymmetric form of the material point method with applications to upsetting and Taylor impact problems. Computer Methods in Applied Mechanics and Engineering, 139(1–4), pp.409–429.